# Initial Evaluation of Processing Methods for an Epsilon Metal Waste Form

## Fuel Cycle Research & Development

***Prepared for***
***U.S. Department of Energy***

*J. V. Crum, D. M. Strachan, M. Zumhoff*
***Pacific Northwest National Laboratories***

***May 2012***

FCR&D-SWF-2012-000108
PNNL-21350

# SUMMARY

During irradiation of nuclear fuel in a reactor, the five fission product elements—Mo, Pd, Rh, Ru, and Tc—migrate to the fuel grain boundaries and form small metal particles of an alloy known as epsilon metal (ε-metal) sometimes called "the five metal phase." When the fuel is dissolved in a reprocessing plant, a significant fraction of these metal particles remain behind with the residue—the undissolved solids (UDS). Some of the same metals that comprise this alloy are dissolved into the aqueous stream (either because they didn't form the ε-metal phase in the fuel or because some of the ε-metal phase dissolved). These metals limit the waste loading in the borosilicate high-level waste (HLW) glass. Epsilon metal is being investigated as a waste form for the five metals from a number of waste streams in the aqueous reprocessing of used nuclear fuel: 1) the ε-metal from the UDS; 2) soluble Tc (removed from solution by ion-exchange); and 3) soluble noble metals (removed from the HLW raffinate by electrochemically). Separate immobilization of these metals has benefits other than allowing an increase in the glass waste loading. These materials are quite resistant to dissolution (corrosion) and survived the chemically aggressive conditions in the fuel dissolver. Remnants of ε-metal particles have survived in the geologically natural reactors found in Gabon, Africa, indicating they have sufficient durability to survive for ~ 2.5 billion years in a reducing geologic environment. Additionally, ε-metal can be made without additives and incorporate sufficient foreign material (oxides) that are also present in the UDS.

Although ε-metal is found in fuel and Gabon, Africa, as small particles (~10 μm in diameter) and has survived intact, an ideal waste form is one in which the surface area is minimized. Therefore, the current effort in developing ε-metal as a waste form is to demonstrate a process to consolidate the particles into a monolith in a cost effective, reliable, manner. Individually, these metals have high melting points (2617 °C for Mo to 1552 °C for Pd) and the alloy is also expected to have a high melting point, possibly exceeding 1500 °C. The purpose of the work detailed in this report is to find a potential commercial process with which ε-metal plus other components of UDS can be consolidated into a solid with minimum surface area and high strength. This reports documents the results from the preliminary evaluation of spark-plasma sintering (SPS), hot-isostatic pressing (HIP), and microwave sintering (MS).

Because bulk ε-metal is not available and vendors could not be identified to make samples of the radioactive ε-metal, the team prepared mixtures of the five individual metal powders using Re as a surrogate for Tc (Mo, Ru, Rh, Pd, and Re). The team also added varying amounts of $ZrO_2$ (0, 17.5, and 35 mass %) to the mixture of five metals to simulate the oxides present in UDS. These mixtures were send to vendors who processed them by SPS, HIP, and MS. The processed samples were then evaluated at Pacific Northwest National Laboratory for bulk density and phase assemblage with X-ray diffraction and phase composition with scanning electron microscopy. Physical strength was only qualitatively evaluated.

Results of these scoping tests showed that nearly full density cermets (ceramic-metal composite) were produced with SPS and HIP with up to 35 mass % of $ZrO_2$. Bulk density of the SPS samples ranged from 87 to 98% of theoretical density, while HIP samples ranged from 96 to 100 % of theoretical density. Microwave-sintered samples containing $ZrO_2$ had low densities of 55 to 60 % of theoretical density.

Structurally, the cermet samples showed that the individual metals alloyed in to the ε-phase (hexagonal-close-packed) alloy (4 – 95 mass %) —the same crystal structure as ε-metal, α-phase (face-centered-cubic) alloy (3 – 86 mass %), while $ZrO_2$ remained in the monoclinic structure of baddeleyite.

Elementally, the samples appeared to have nearly uniform composition, but with some areas rich in Mo and Re, the two components with the highest melting points. The homogeneity in distribution of the elements in the alloy is significantly improved in the presence of $ZrO_2$. However, $ZrO_2$ does not appear to react with the alloy, nor was Zr found in the alloy.

From these test results, the team concludes that both HIP and SPS technologies can be used to produce an ε-metal waste form, with and without $ZrO_2$. Microwave sintering can be used to produce ε-metal phase alone, but added $ZrO_2$ results in low density materials with poor mechanical strength.

# CONTENTS



# FIGURES

## TABLES

# ACRONYMS

| | |
|---|---|
| CETE | coupled-end-to-end |
| EDS | energy dispersive spectroscopy |
| HIP | hot-isostatic pressing |
| HLW | high-level waste |
| MS | microwave sintering |
| PVA | polyvinyl alcohol |
| SEM | scanning electron microscopy |
| SPS | spark-plasma sintering |
| UDS | undissolved solids |
| XRD | X-ray diffraction |
| ε-metal | epsilon-metal (alloy of Mo, Ru, Rh, Pd, and Re) with hexagonal-close packed structure |
| α-metal | alpha-metal (alloy of Mo, Ru, Rh, Pd, and Re) with face-centered-cubic structure |

# 1. INTRODUCTION

During irradiation of nuclear fuel in a reactor, the five fission product elements—Mo, Pd, Rh, Ru, and Tc—migrate to the fuel grain boundaries to form small metal particles of an alloy known as epsilon metal (ε-metal) (Kleykamp 1987, 1988). When the fuel is dissolved in a reprocessing plant, these metal particles remain behind with the undissolved solids (UDS). A portion of the metals that comprise this alloy are dissolved into the aqueous stream either because they did not form ε-metal or because a portion of the ε-metal dissolved. These dissolved metals or combination of dissolved metals plus UDS limit the waste loading for a borosilicate glass high-level waste (HLW) form. To immobilize these metals—primarily the $^{99}$Tc with a 213,000 y half-life—an iron-based alloy waste form (Ebert et al. 2009b; Ebert et al. 2010) and ε-metal are being developed. For the iron-based alloy waste form, the ε-metal particles and metals separated from the aqueous process are melted with stainless steel to form an ingot (Ebert et al. 2009b; Ebert et al. 2010).

In the ε-metal waste form, the particles in the UDS and the metals separated from the aqueous process are consolidated without any additions. Metals from a number of waste streams in the aqueous reprocessing of used nuclear fuel are included: 1) the ε-metal formed during fuel irradiation (found in the UDS); 2) soluble Tc (removed from aqueous solution by ion-exchange); and 3) soluble noble metals (removed from the HLW raffinate electrochemically). Separate immobilization of these metals has benefits other than allowing an increase in the glass waste loading. These materials are resistant to dissolution (corrosion) as evidenced by the fact they survived the chemically aggressive conditions in the fuel dissolver. Remnants of ε-metal particles have also survived in the geologically natural reactors found in Gabon, Africa, indicating they possess sufficient durability to survive for ~ 2.5 billion years in a reducing geologic environment. In addition, the ε-metal can be made without additives and incorporate sufficient oxide impurities that are present in the UDS.

The dissolved fractions of these five metals are problematic for treatment of wastes from aqueous processing. Because the noble metals (Pd, Rh, and Ru) have low solubility in borosilicate glasses, they limit the waste loading. Molybdenum is troublesome in borosilicate glass because it tends to form a separate liquid phase. However, molybdenum can be immobilized in a glass ceramic by crystallizing it into a durable phase (powellite). Technetium can be oxidized to $Tc^{7+}$, which volatilizes as an oxide or alkali-pertechnetate at temperatures below 450 °C, making it difficult to retain in borosilicate glass melts. For these reasons, it is generally assumed a better option to remove these metals from the overall waste stream and immobilize them separately from the reference borosilicate glass or glass ceramic. Of the metals that need to be treated separately, Zr is the only one that is very difficult to reduce to the metallic form. Thus, it is likely it will be incorporated as $ZrO_2$. An option for the immobilization of these metals is processing them into ε-metal phase, incorporating the Zr as $ZrO_2$.

Strachan et al. (2010) and Ebert et al. (2010) independently demonstrated the ε -metal waste form can easily be produced by arc melting. However, product from arc melting does not appear to have good strength when oxides are present because of their very different melting properties compared to metals. Additionally, arc melting is known to cause volatility of some alloy component (e.g., Pd). Arc melting was not ranked very favorably by Rohatgi and Strachan (2011) when compared with other processes. For this reason, other technologies need to be considered for producing the ε -metal plus oxide "cermet" waste form. Rohatgi and Strachan identified microwave sintering (MS), spark plasma sintering (SPS), and hot-isostatic pressing (HIP) as the three commercially available processes most likely to successfully process ε-metal waste form in a reprocessing facility.

If voloxidation is performed as part of the separations process, especially high-temperature voloxidation (> 800 °C), then more oxides are present. During high-temperature voloxidation, most—if not all—of the ε-metal is oxidized (Strachan et al. 2011). The resulting oxides of these metals are still expected to cause

difficulties in processing of a single borosilicate high-level waste form. Thus, it is advantageous to process these oxides into a separate ε-metal waste form from the aqueous process.

Of the oxides making up the UDS, $ZrO_2$ is the only element not reducible to metal, by common methods in literature (Kan et al. 2008; Schulmeyer and Ortner 2002; Suhonen et al. 2002; Prudenziati et al. 2003; Orehotsky and Kaczenski 1979; Ebert et al. 2009a). For the purpose of this study, team members assume that all components other than $ZrO_2$ will be reduced to metals. Because ε-metal contains all of the metals in these problematic waste streams and $ZrO_2$ may be present as an oxide or a molybdate that can be reduced, a viable process is likely to be one in which ε-metal can be consolidated with $ZrO_2$ to form a physically strong cermet monolith. Chemically, this material should be quite durable because the ε-metal appears to have a proven longevity from studies of the natural reactors in Gabon, Africa (Gauthier-Lafaye et al. 1996; Utsunomiya and Ewing 2006). The $ZrO_2$ is very insoluble and contains no isotopes with long-term implications to waste form performance ($^{93}Zr$ [$t_{1/2} = 1.53 \times 10^6$ y] is immobile in all geological settings).

Although ε-metal is found in fuel and Gabon, Africa, as small particles (~10 μm in diameter) (Utsunomiya and Ewing 2006) that have survived intact, an ideal waste form is one in which the surface area is minimized. Therefore, the current effort in developing ε-metal as a waste form is in developing and demonstrating a process to consolidate the particles into a monolith. Individually, these metals have high melting points (2617 °C for Mo to 1552 °C for Pd) and the alloy is expected to have a high melting point as well, perhaps exceeding 1500 °C. The purpose of the work reported here is to find a potential commercial process with which ε-metal plus other components of UDS can be consolidated into a solid with minimum surface area and high strength. Here, the team reports the results from the initial demonstration tests using SPS, HIP, and MS.

Because bulk ε-metal is not readily available, the team prepared mixtures of the five individual metal powders with Re as a surrogate for Tc (Mo, Ru, Rh, Pd, and Re). Variable concentrations of $ZrO_2$ (0, 17.5, and 35 mass %) were added to the mixture of metal powders in the form of baddeleyite with selected samples containing yittryia stabilized zirconia (YZS). Last fiscal year, available consolidation technologies were examined and ranked in terms of chance of success, cost, and maturity (Rohatgi and Strachan 2011). The processed samples were then evaluated at Pacific Northwest National Laboratory for bulk density and phase assemblage by scanning electron microscopy (SEM) and X-ray diffraction (XRD). Physical strength was evaluated qualitatively.

For this study, the team focused on the process to consolidate the five individual metals with the addition of $ZrO_2$. Thus, a successful outcome of this testing is a monolithic material with a reasonable physical strength—one in which the surface area of the ε-metal is reduced relative to that of 10-μm particles. Given that small ε-metal particles (sub-millimeter) have been demonstrated to remain nearly immobile over long geologic time periods (Utsunomiya and Ewing 2006), a fully dense waste form is not necessary from a waste performance standpoint, but rather the waste form needs to consolidated and maintain strength for handling, and transport.

## 2. Simulated Waste Composition

The simulated waste stream and consequent range of $ZrO_2$ was calculated from the two extremes for $ZrO_2$ content in the projected waste stream, as shown in Table 1. The elemental concentrations were calculated based on the results of the four-corners study (Vandegrift 2009) (define the effect of nuclear fuel burn up and decay time) and available separations data for aqueous reprocessing. A combination of low burn up fuel (25 GWd) and the results of the coupled-end-to-end (CETE) separations testing by Benker et al. (2008) defines the minimum $ZrO_2$ (3.7 mass %) and the combination of high burn up fuel (100 GWd) and the report by Bakel et al. (2006) defines the maximum projected concentrations $ZrO_2$ (35.0 mass %) considered for this work. Other oxides, such as $PuO_2$, were excluded for this study and the composition renormalized, where Re was substituted for Tc on an equimolar basis. The concentrations of the metals—

Mo, Re, Ru, Rh, and Pd—were selected to match the previous ε-metal waste form development work. Based on this, three levels of $ZrO_2$ (0, 17.5 and 35.0 mass %) were selected for testing.

Table 1. Projected waste and fiscal year 2012 target compositions (mass %).

| Burn-up and Decay | 25 GWd-5yr | 100 GWd-50yr | | | | |
|---|---|---|---|---|---|---|
| Separations Variability | CETE | Bakel et al. (2006) | | Baseline | Base + 17.5 $ZrO_2$ | Base + 35 $ZrO_2$ |
| Range | min $ZrO_2$ | max $ZrO_2$ | | | | |
| $ZrO_2$ | 3.7 | 35.0 | | 0 | 17.5 | 35.0 |
| Mo | 10.5 | 22.6 | | 35.4 | 29.2 | 23.0 |
| Re | 20.8 | 10.0 | | 17.2 | 14.2 | 11.2 |
| Ru | 35.0 | 18.2 | | 28.0 | 23.1 | 18.2 |
| Rh | 8.4 | 2.4 | | 4.7 | 3.9 | 3.1 |
| Pd | 21.6 | 11.8 | | 14.7 | 12.1 | 9.6 |
| Total | 100.00 | 100.0 | | 100.0 | 100.0 | 100.0 |
| CETE = Coupled-end-to-end; GWd = gigawatt/day | | | | | | |

## 3. Experimental

Samples of the five individual metals—Mo, Ru, Rh, Pd, and Re (Tc surrogate) —plus baddeleyite ($ZrO_2$) were weighed out in powder form (~325 mesh) on a balance with a precision of ±0.2 mg. Powder batches were homogenized with a vortex mixer. Polyvinyl alcohol (PVA) was added as a binder when preparing pellets.

MS and SPS samples were pressed into 15-mm diameter pellets with cold-isostatic pressing to a pressure of ~340 MPa. The PVA binder was burned out of the pellets by heating to 200 °C and held for 4 hr, further heating to 600 °C and held for 0.5 hr in flowing nitrogen before being sent to vendors of SPS and HIP. During microwave heating, the binder was burned out during the process. The HIP samples were prepared by loading mixed but unconsolidated powders into evacuated and sealed metal foil envelopes.

### 3.1 Spark Plasma Sintering Process

Pellets were sent to the California Nanotech Corporation (Cerritos, California) for processing in its laboratory-scale spark-plasma instrument. Pellets were wrapped in graphite foil and loaded into a graphite die. The samples were rapidly heated to 800 °C at ~260 °C/min, and then to ~1525 °C at 100 °C/min briefly to soften the material and start the alloy process. The temperature was then decreased to 1500 °C and held for 20 or 40 minutes to complete the alloying and consolidation processes. They were cooled to 1000 °C at ~50 °C/min, then to 650 °C at ~90 °C/min at which point the power to the furnace was turned off. Pressure was applied beginning at ~1190 °C at a rate of ~2.9 kN/min up to a maximum of 14.5 kN (70 MPa with 15 mm die) at 1525 °C and held at that pressure during ≥1500 °C steps. The pressure was reduced at a rate of 1.13 kN/min as the sample cooled. Figure 1a shows the

temperature, pressure, and displacement with time for a sample 17.5%$ZrO_2$-SPS-1-2012 and 35%$ZrO_2$-SPS-1-2012 and Figure 1b shows the temperature, applied current, and applied voltage for the same runs (samples) with a 20-min hold at the sintering temperature. The process took a total of 45–65 min per sample.

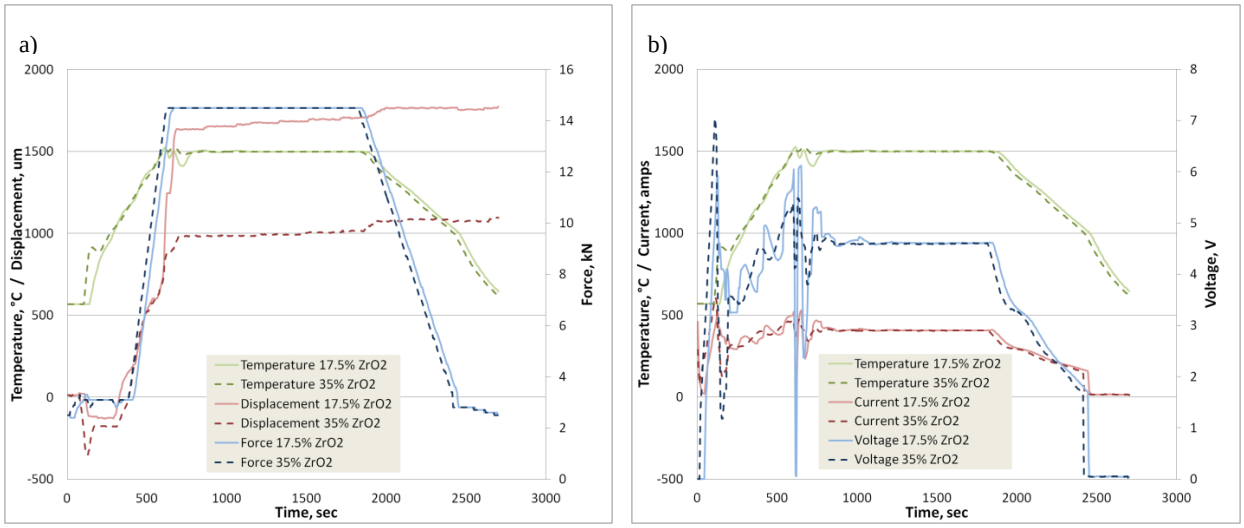


Figure 1. Spark-plasma processing conditions (temperature, displacement, force, current and voltage as a function of time) for samples 17.5%$ZrO_2$-SPS-1-2012 and 17.5%$ZrO_2$-SPS-1-2012.

## 3.2 Hot-Isostatic Pressing Process

Powders were placed onto either zirconium or tantalum, 0.013-mm (0.0005”) foils, evacuated to approximately 0.01 Pa ($10^{-4}$ torr), and sealed with electron-beam welding (Figure 2). Packages were prepared in three steps: 1) three sides of the package were welded with an electron-beam welder; 2) sample powder was added; and 3) the fourth side was electron-beam welded (sealed). A copper clamp was used to hold tantalum foil during electron-beam welding to avoid overheating the foil and sample and causing warping and failed welds.

Figure 2. Typical hot-isostatic press package, Zr foil envelope shown, filled with sample powder before press processing.

Sealed packages were sent to American Isostatic Pressing (Columbus, Ohio) for HIP processing in its research-scale HIP. The HIP has carbon heating elements and argon gas to pressurize the chamber. The samples were rapidly heated to 1500 °C and held for 1hr at a pressure of 207 MPa; Figure 3 shows the temperature and pressure profiles.

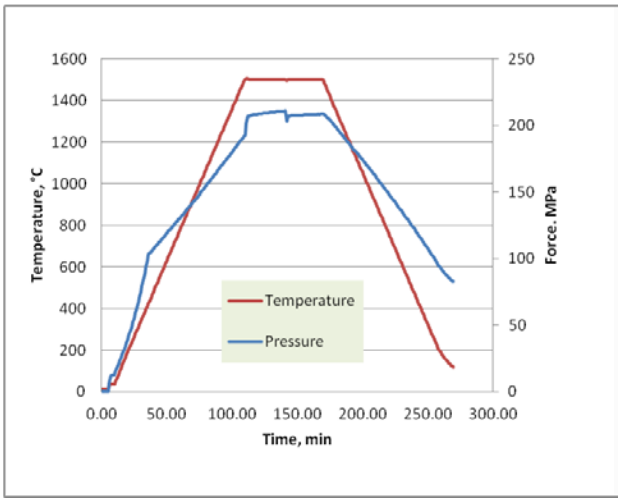


Figure 3. Hot-isostatic pressing processing conditions (temperature, pressure).

## 3.3 Microwave Sintering Process

Samples were sent to Spheric Technologies, Inc. (Phoenix, Arizona) for processing with MS. The sample pellets were loaded onto silicon carbide sinter plates and placed into the microwave chamber. The chamber was evacuated and backfilled three times with argon. The samples were then processed in flowing argon with the following temperature cycle:

- Manual control set to 460 °C and held for 2 min (binder burnout)
- Ramp set to 475 °C at 1.5 °C/h and held 30 min (binder burnout)
- Ramp set to 1550 °C at 17 °C/min and held 120 min (processing temperature).

## 3.4 Sample Characterization

After processing with SPS, HIP, or MS the samples were cut and polished for measurement of bulk density by the Archimedes method, and phase analysis using both XRD and SEM energy dispersive spectroscopy with elemental analysis.

Density was measured in ethanol with the Archimedes method. First, samples were weighed on a balance accurate to ±0.2 mg. Samples were then submerged in ethanol and subjected to a laboratory vacuum to allow the ethanol to penetrate any open porosity. Next, the samples were weighed both suspended in ethanol and in air saturated with ethanol. The temperature of the ethanol was monitored to determine its density ($\rho_{EtOH} = -8.54\times10^{-4}*T + 0.806$, where temperature, $T \sim 15–25°C$) (*Standard Density and Volumetric Tables* 1924). Bulk density was calculated according to Equation (1):

$$\rho_{sample} = \frac{\left(x_{dry} \bullet \rho_{etoh}\right)}{\left(x_{sat} - x_{sub}\right)} \qquad (1)$$

Where $x_i$ is the mass in the ith configuration ($i$ = dry, saturated/suspended, and submerged respectively), $\rho_{etoh}$ is the calculated density of ethanol at temperature of the test. Open porosity was also calculated according to Equation (2):

$$OpenPorosity = \frac{\left(x_{sat} - x_{dry}\right)}{\left(x_{sat} - x_{sub}\right)} \quad (2)$$

### 3.4.1 X-ray Diffraction

XRD patterns were collected on polished sample surfaces from 20–110° 2θ at a step size of 0.015° 2θ and at a rate of 1.5 s/step. The diffractometer had a Cu-X-ray tube and a one-dimensional detector with a collection angle of 3° 2θ. The samples were rotated during the measurements to minimize the effects of preferred orientation. Phase analyses were done with Rietveld refinement using TOPAS 4.2 software, according to the fundamental parameters approach to determine the phase assemblage. It was not possible to prepare homogenous powder samples because the ε-metal cannot be ground and is too hard to file. Therefore, XRD scans are snap shots of the cross-sectioned polished surface instead of the preferred bulk analysis typically achieved by X-ray powder diffraction.

### 3.4.2 Scanning Electron Microscopy

Cross-sectioned samples were examined with SEM and energy dispersive spectroscopy to determine the extent to which the starting materials reacted, the porosity, and the character of grain boundaries. Uncoated samples were used for SEM specimens and the SEM was operated in both high and low vacuum modes at an accelerating voltage of 6 kV to minimize beam penetration depth. With low electron beam penetration depth, elemental analyses and imaging resolution are improved. Backscattered electron imaging was used to show changes in atomic number ($Z$), revealing any differences in chemistry. Elemental spot analyses were collected for both the metal and oxide phases. Elemental dot maps were also collected to reveal the distribution of individual elements throughout the metal phase.

# 4. Results

## 4.1 Spark Plasma Sintering

The melting point of the ε-metal alloy was unknown. Thus, the first sample was heated to a target temperature of 1750 °C. This process resulted in the pellet being extruded from the graphite die at ~1650 °C because it melted. However, the failed test clearly showed that between 1500 °C and 1525 °C, the pellet softened and began to flow, making 1500 °C to 1525 °C a good temperature range at which to perform the next attempt. All other tests were run at a soak temperature of 1500 °C for 20–40 min, which achieved good densification. However, hold times of 40 min allowed the alloy to seep through the protective graphite foil and stick to the graphite die set, shortening the die life. Successive tests were performed with a 20-min hold at 1500 °C. This worked well for alloying the individual metals without affecting the graphite die.

The SPS samples have measured densities from 90% to 98% of the calculated theoretical densities (unit cell calculated density), which depends on the fraction of $ZrO_2$ present (Table 2). The measured open porosity was ~ 2.5% and the porosity in the bulk was found to be ~4.5% with image analysis (Figure 4). The vast majority of porosity observed under the microscope was between the $ZrO_2$ grains and not in the metal alloy.

XRD of the polished pellets showed the presence of three major phases: α-phase [face-center-cubic (FCC)] metal alloy, ε-phase [hexagonal-close-pack (HCP)] metal alloy, baddeleyite ($ZrO_2$), and a minor phase of molybdenum carbide (Table 3). Samples that contained $ZrO_2$ had higher contents of the ε-metal alloy than samples that contained only the five metals, in which more of the α-metal phase was present.

Figure 5 shows an XRD pattern with the phase identities—the pattern shows dominant HCP ε-alloy, followed by $ZrO_2$, $Mo_2C$, and the FCC α-alloy. Figure 6 shows an elemental dot map of this sample, confirming the XRD results. Although not detected with the phase analysis of the dot map, there is evidence of a second phase on the upper right-hand side of the backscattered electron (BSE) image in Figure 6. Spot analysis of the small grey slivers reveals they are higher in Mo than the bulk metal alloy. This may be the molybdenum carbide observed in the XRD pattern. The darker gray area at the left (alloy grain) of the BSE image in Figure 6 is likely an effect of grain origination (epsilon is an HCP structure).

Table 2. Measured density, open porosity, measured theoretical, and percent of calculated theoretical density.

| Sample Name | Firing Temperature, Soak Time, Pressure | Bulk Density g/cm$^3$ | Open Porosity (%) | True Density[1] g/cm$^3$ | Theoretical[2] (%) |
|---|---|---|---|---|---|
| BL-SPS-1-2012 | Extruded from die at 1650 °C, 70 MPa | 10.64 | 2 | 10.86 | 87 |
| 17.5% $ZrO_2$-SPS-1-2012 | 1525 °C bump, 1500 °C-20 min, 70 MPa | 9.85 | 2 | 10.09 | 89 |
| 35% $ZrO_2$-SPS-1-2012 | 1525 °C bump, 1500 °C-20 min, 70 MPa | 8.45 | 3 | 8.68 | 87 |
| BL-SPS-2-2012 | 1525 °C bump, 1500 °C-40min, 70 MPa | 11.48 | 2 | 11.68 | 94 |
| 17.5% $ZrO_2$-SPS-2-2012 | 1525 °C bump, 1500 °C-40min, 70 MPa | 9.77 | 3 | 10.03 | 88 |
| 35% $ZrO_2$-SPS-2-2012 | Die failed at 1400 °C, 70 MPa | NA | -- | -- | -- |
| BL-SPS-YSZ-3-2012 | 1525 °C bump, 1500 °C-20 min, 69 MPa | 12.02 | 1 | 12.09 | 98 |
| 17.5% $ZrO_2$-SPS-YSZ-3-2012 | 1525 °C bump, 1500 °C-20 min, 69 MPa | 10.19 | 0 | 10.21 | 92 |
| 35% $ZrO_2$-SPS-YSZ-3-2012 | 1525 °C bump, 1500 °C-20 min, 69 MPa | 8.61 | 1 | 8.69 | 89 |
| BL-HIP-1-Ta-2012 | 1500 °C-1hr, 207 MPa | 11.09 | 1 | 11.16 | 91 |
| 35%$ZrO_2$-HIP-1-Ta-2012 | 1500 °C-1hr, 207 MPa | 10.94 | 5 | 11.54 | 113 |
| BL-$ZrO_2$-microw-3-2012 | Melted and reacted with sinter plate | NA | | | |
| 17.5% $ZrO_2$-microw-3-2012 | 1550 °C-2hr, 1 ATM argon | 6.07 | 35 | 9.40 | 55 |
| 35% $ZrO_2$-microw-3-2012 | 1550 °C-2hr, 1 ATM argon | 5.95 | 12 | 6.77 | 61 |

[1]True density = bulk density/(100% - open porosity).
[2]Theoretical = Calculated density based on target epsilon and $ZrO_2$ concentrations.

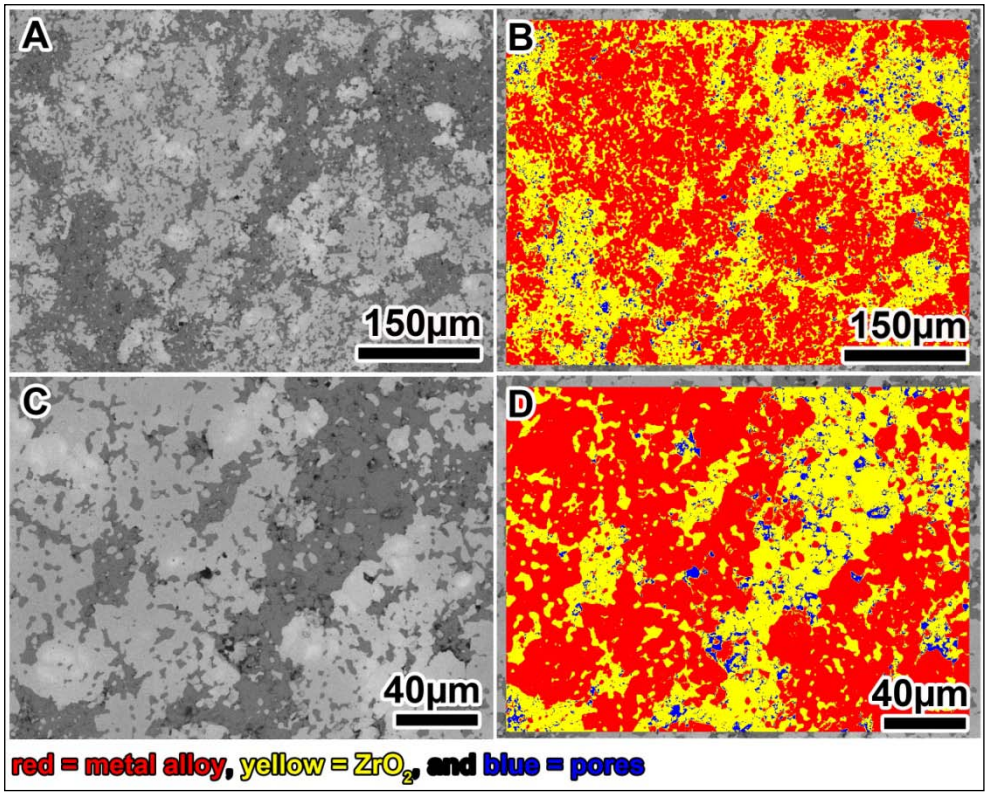


Figure 4. Image analysis of 17.5%$ZrO_2$-SPS-1-2012 scanning electron microscopy backscattered electron micrographs showing area% metal alloy, $ZrO_2$ and porosity: A) 200× backscattered electron, B) 200× phases colored, C) 500× backscattered electron, and D) 500× phases colored. Pores = 4.5 vol%.

These results show excellent consolidation of the cermet using the spark plasma sintering process, considering only 10 samples have been run to date (including 3 metal-only samples last year). The team concludes that spark plasma sintering can be used to process the ε-metal alloy with and without $ZrO_2$.

Table 3. Semiquantitative phase analysis by X-ray diffraction, mass% (monolith samples)

| Sample ID | Conditions – Temperature, Soak, Time, and Pressure | Epsilon (Hex) | Epsilon (Cubic) | $ZrO_2$ | $Mo_2C$ |
|---|---|---|---|---|---|
| 17.5% $ZrO_2$-SPS-1-2012 | 1500 °C/20 min/70 MPa | 47.5 | 18.8 | 29.8 | 3.9 |
| 35% $ZrO_2$-SPS-1-2012 | 1500 °C/20 min/70 MPa | 24.5 | 24.8 | 39.4 | 11.4 |
| BL-SPS-2-2012 | 1500 °C/40 min/70 MPa | 9.4 | 85.7 | - | 4.9 |
| 17.5% $ZrO_2$-SPS-2-2012 | 1500 °C/40 min/70 MPa | 63.9 | 3.1 | 26.5 | 6.5 |
| BL-SPS-YSZ-3-2012 | 1500 °C/20 min/69 MPa | 14.4 | 80.6 | - | 5.0 |
| 17.5% $ZrO_2$-SPS-YSZ-3-2012 | 1500 °C/20 min/69 MPa | 4.2 | 66.9 | 26.6 | 2.3 |
| 35% $ZrO_2$-SPS-YSZ-3-2012 | 1500 °C/20 min/69 MPa | -- | -- | -- | -- |
| BL-HIP-1-Ta-2012 | 1500 °C/60 min/207 MPa | 95.1 | 4.9 | 0 | 0 |
| 35% $ZrO_2$-HIP-1-Ta-2012 | 1500 °C/60 min/207 MPa | 49.7 | 5.1 | 45.2 | 0 |

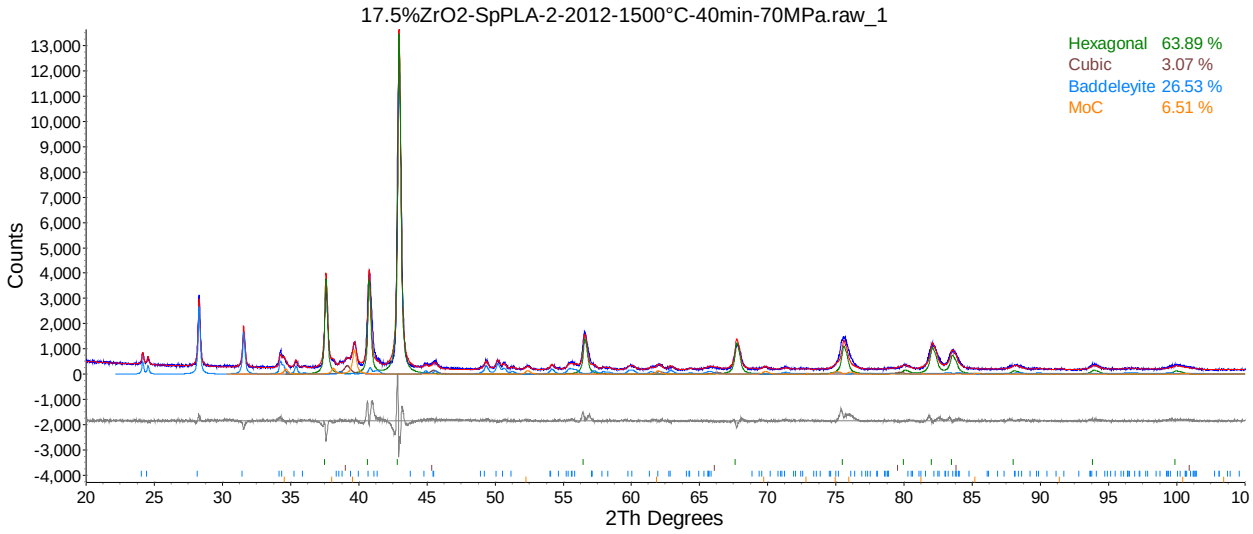


Figure 5. X-ray diffraction of 17.5% $ZrO_2$ composition processed by spark plasma sintering at 1500 °C, 40 min, 70 MPa (monolith sample).

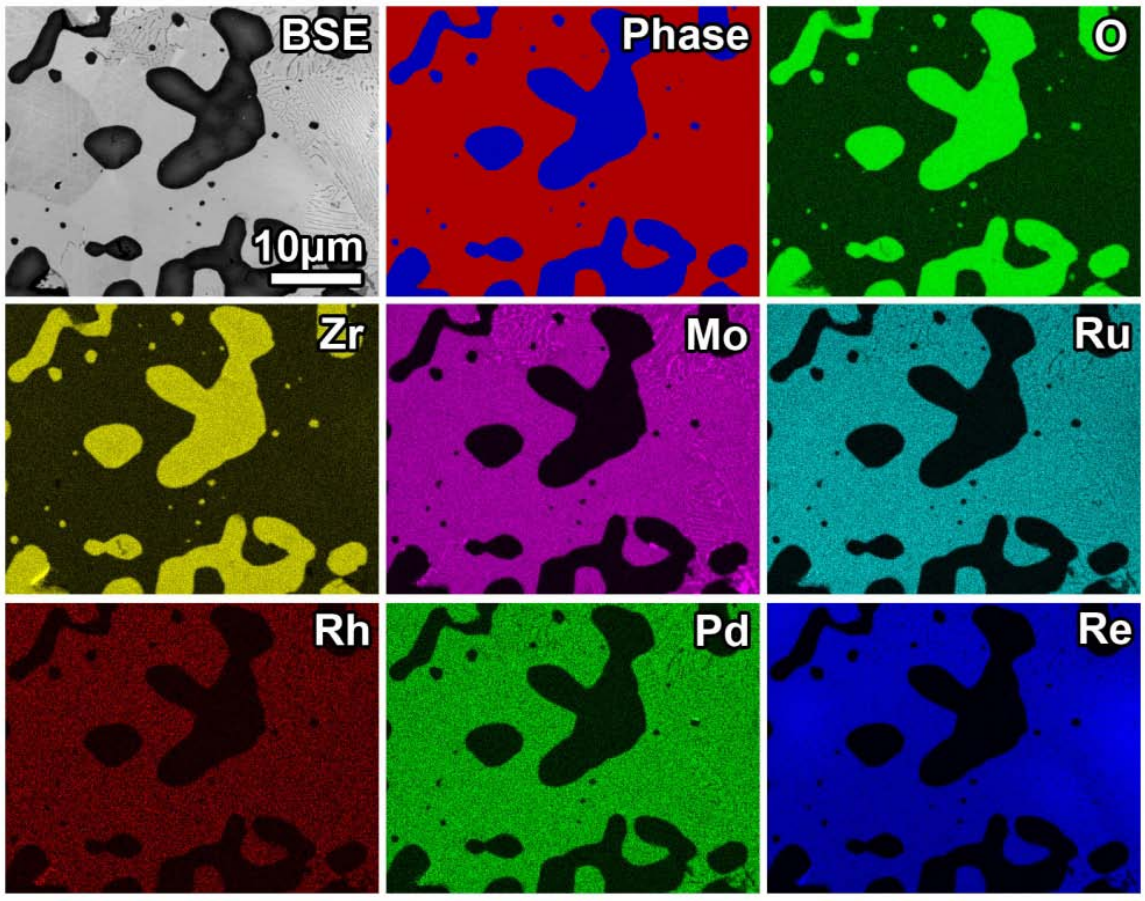


Figure 6. Elemental dot map of 17.5%$ZrO_2$-SPS-2-2012 (1500 °C, 40 min, 70 MPa) showing epsilon phase (red) and $ZrO_2$ (blue) on phase map.

## 4.2 Hot-Isostatic Pressing

Results from HIP processing are limited compared to SPS, because of time consumed designing and preparing the HIP packages. Two metal foils, Zr and Ta, were selected for the HIP packages. Zirconium foil appears to react on the outside with carbon from the heating elements in the HIP chamber and the ε-metal alloy on the inside. Conversely, Ta foil was much less reactive on the inside and outside. However, Ta is less pliable and less thermally conductive (requiring a copper clamp when welding). On the whole, the non-reactivity of Ta was found to outweigh the shortcomings. Ta foil was used in the remaining tests.

Measured densities of the HIP samples are slightly higher than the densities achieved with the SPS. The samples processed with HIP were >90% of theoretical density. Note the density was measured with the Ta foil package attached because of the small sample size and the difficulty separating the Ta foil from the sample. The mass and density of the Ta foil were known so the overall density of the sample plus Ta foil was measured and the contribution of the Ta foil was accounted in the calculation of the HIP samples density. Because of this correction, there is some added error in the density measurements of the HIP samples.

Semiquantitative XRD results (Table 3) for the baseline and 35% $ZrO_2$ HIP samples show that both samples contain ε-metal HCP as the dominant alloy, a small fraction of the α-metal FCC alloy, Ta metal belonging to the HIP package, and amorphous humps centered near 30° and 42° 2θ from the epoxy mount (Figure 7 and Figure 8). Overall, results are excellent considering the starting material is the individual metals and only two HIP samples were run. In the SEM, the ε-metal alloy appears similar to those produced with SPS. Figure 9 shows micrographs taken with BSE imaging at the interface between the sample and Ta-foil at (A) 150×, center region at magnifications of (B) 150×, (C) 500× , and (D) 5000×.

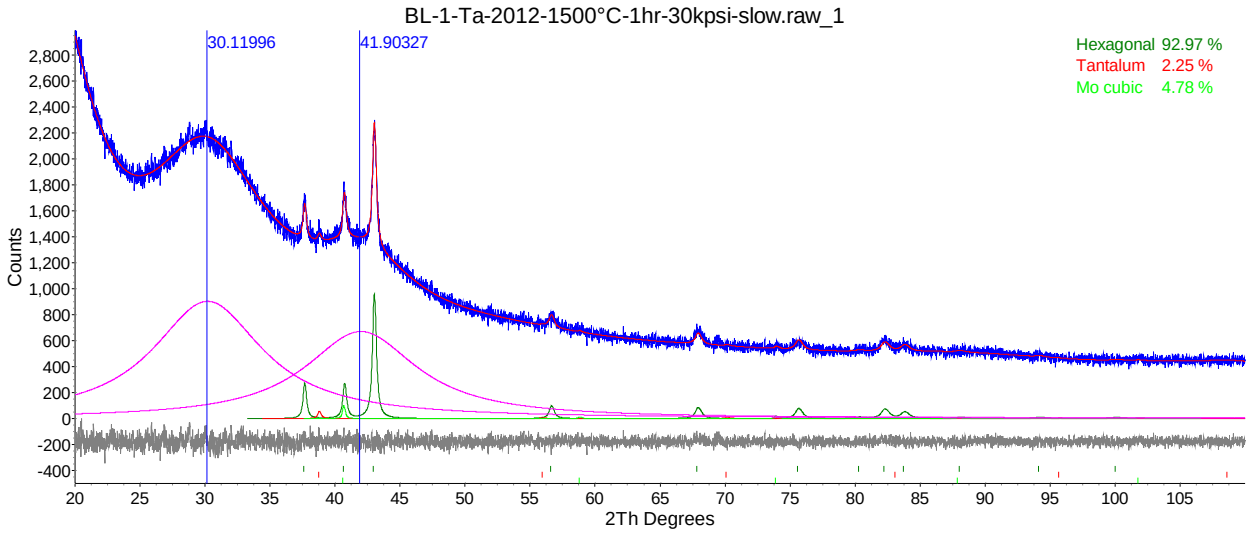


Figure 7. X-ray diffraction pattern of BL-HIP-1-Ta-2012 processed by hot-isostatic press at 1500 °C, 1hr, 207 MPa (amorphous humps in background due of epoxy mount).

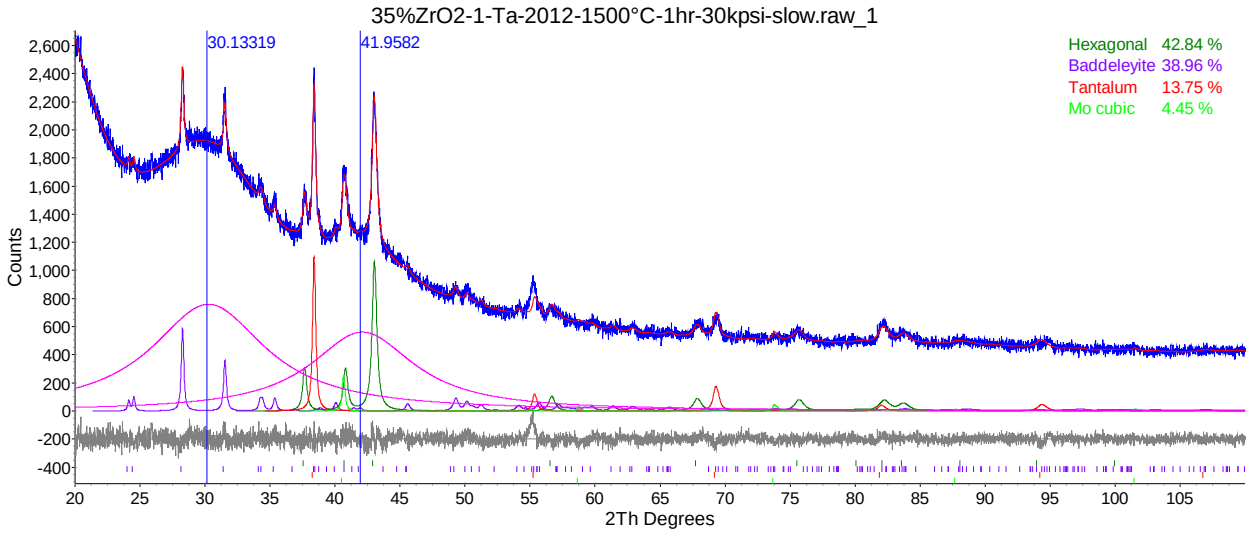


Figure 8. X-ray diffraction pattern of 35%$ZrO_2$-HIP-1-Ta-2012 processed by hot-isostatic press at 1500°C, 1 hr, 207 MPa (amorphous humps in background due of epoxy mount).

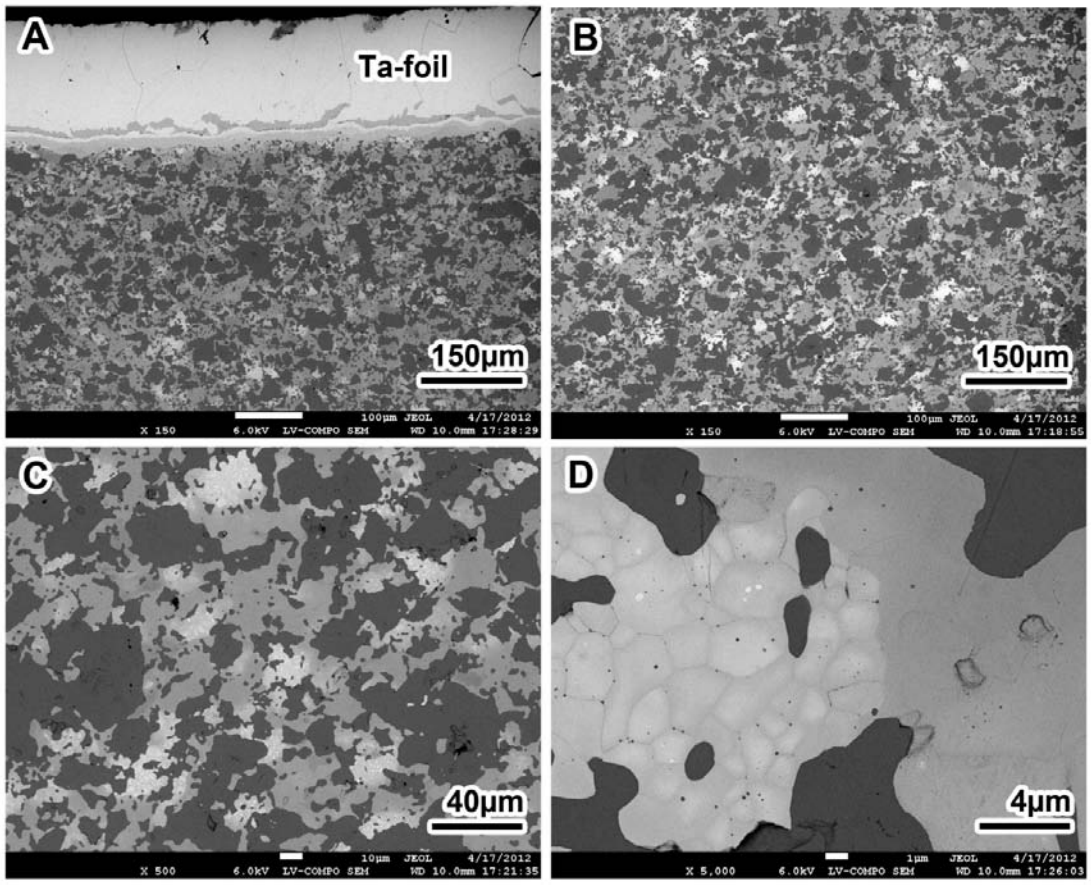


Figure 9. Electron backscattered image of 35%$ZrO_2$-HIP-1-Ta-2012 sample at 1500 °C, 1hr, 207 MPa in Ta-foil package.

There is a small interface (~ 10µm) between the Ta foil and ε-metal that shows a small amount of alloying occurs between the package and the sample. The dark grey areas are $ZrO_2$, the light grey is the metal alloy, and black is porosity. The lighter and a darker grey areas within the metal alloy are areas that contain higher concentrations of Re and Mo relative to the bulk alloy composition. The alloying looks less complete elementally than SPS, which indicates that HIP processing temperatures could be slightly higher. However, the XRD results show the HCP structure is more dominant than in the SPS samples. Further testing is needed to identify the proper temperatures for HIP and SPS, but these preliminary results show that both processes produce similar products with high densities.

## 4.3 Microwave Sintering

Last fiscal year, microwave sintering was shown to produce ε-metal (without $ZrO_2$) at ~1500 °C for ~45 min. However, the density was poor (57% of theoretical density). This year, the processing temperature was increased to 1550 °C and hold time to 120 min in an effort to increase the density. The ε-metal melted and formed a puddle on the silicon carbide sinter plate. Thus, the microwave oven is capable of melting and alloying the ε-metal after a suitable crucible is identified to handle both the microwave process and the metal alloy.

However, when $ZrO_2$ is added at 17.5 or 35 mass% to the material, it behaved differently than metal only. Figure 10 shows photographs of two pellets containing $ZrO_2$ at 17.5 and 35 mass%. The pellets contain significant fracturing, likely from thermal gradients. The center portion of the 35% $ZrO_2$-Microw-3-2012 pellet completely separated from the outer edges and top of the pellet, as seen in Figure 10 (left), the arrow showing where the center portion was when the sample was removed from the furnace.

The measured densities are very low at ~60% of theoretical density. Because of the low density and fracturing, no further analyses of the MS samples were done for this report. This does not preclude MS from being a good choice at a later date for processing the cermet waste form, but these results indicate that more development is needed than for SPS and HIP.

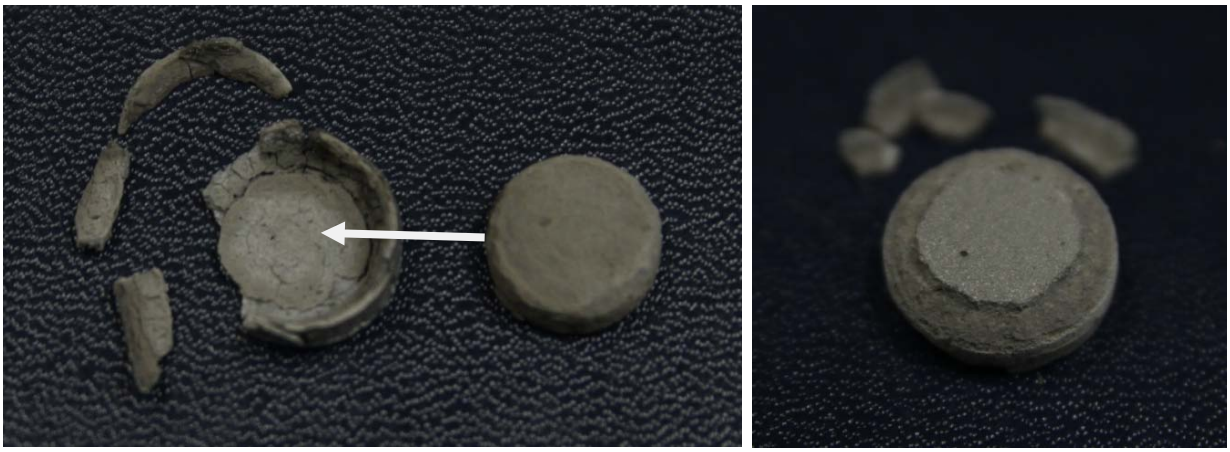

Figure 10. Pellets showing 35%$ZrO_2$-Microw-3-2012 (left) and 17.5%$ZrO_2$-Microw-3-2012 (right) processed at 1550 °C-120 min in argon.

# 5. Conclusions and Recommendations for Future Research

As stated in Section 1, "Introduction," producing the ε-metal alloy with commercially available processes was a primary focus for the current ε-metal waste form development task, especially for samples with significant concentrations of oxides. The results from tests run at three vendor sites clearly show dense monolith forms of ε-metal alloy can be produced with SPS or HIP, with $ZrO_2$ at up to 35 mass%. The

presence of $ZrO_2$ was expected to be a hindrance in the consolidation process, but it appears to only hinder the use of MS while slightly improving the formation of the ε-phase in SPS.

The results in this report were obtained starting with five individual metals (Mo, Ru, Rh, Pd, and Re) instead of the small ε-metal alloy particles that are found in used nuclear fuel. Using these metals resulted in some elemental variability within the samples at the 10-50 μm scale. Making the cermet waste form starting with ε-metal and fabricating the waste form with Tc rather than Re may change the results. It is likely that the results will be better for actual wastes as pre-alloying of the five metals will likely reduce the time required to consolidate and Tc has a significantly lower melting temperature than Re and may react faster. Tests with Re-ε-metal and Tc-ε-metal should be conducted to verify these assumptions.

Further work needs to be performed to optimize one or both the SPS and HIP processes. At this time, there is no need to pick one technology over the other. Each has benefits and drawbacks to consider. Hot-isostatic pressing is well established at all scales. However, it requires a container, such as Ta, in which to densify the waste form. The container needs to be designed to yield a product with reliable shape and dimensions, something that is routinely done in industry. Spark-plasma sintering does not require a container, but rather relies on a die and punch set in which to densify the waste form. However, it is a relatively new technology. Both technologies are possible candidates for processing other waste forms besides the ε-metal; e.g., glass ceramics or ceramics. The HIP may have a slight advantage if multiple waste forms are to be produced because the HIP can is the containment vessel, so cross contamination of wastes is unlikely.

One significant need in this research is bulk quantities of ε-metal powder or simulated UDS for testing processing methods. In the future, a supply of simulated ε-metal particles needs to be fabricated with the five metals to better simulate the waste stream versus batching from the five individual metal powders, which suffers from a wide range of melting temperatures (Pd = 1552 °C to Re = 3180 °C). Second, a systematic test matrix is needed to pinpoint the optimal conditions (temperature and pressure schedule) and materials (HIP package, SPS die and packaging) to produce the cermet waste form by both processes. These tests are needed to establish a typical or reference cermet waste from that can be used to start corrosion testing and determine the characteristic corrosion behaviors of the ε-metal, $ZrO_2$, and overall cermet waste form in applicable disposal environments.

Scale-up testing is critical for the demonstration of either process. One process may be more effective than the other at prototypical scales. However, this would require the use of large quantities of expensive metals. So, timing for such expenditure should be well planned.

The team successfully produced dense, nearly fully reacted (>90% ε-metal HCP alloy), ε-metal containing 0, 17.5, and 35 mass% $ZrO_2$ (as a surrogate for the oxide materials in UDS and Zr that is not easily reduced to Zr metal). Even though the team started with the five individual metals (Mo, Pd, Re, Rh, and Ru), fully dense and reacted metals were produced with SPS and HIP. These are two of the methods identified in an earlier study (Rohatgi and Strachan 2011) as likely processes to produce an ε-metal waste form in a reprocessing facility.

# 6. References

Bakel, AJ, DL Bowers, KJ Quigley, MC Regalbuto, JA Stillman, and GF Vandegrift. 2006. "Dissolution of Irradiated Nuclear Fuel from the Big Rock Point Reactor." In *Separations for the Nuclear Fuel Cycle in the 21st Century*, Vol 933, pp. 71-88. American Chemical Society, Washington, DC.

Benker, D, L Felker, E Collins, P Bailey, and J Binder. 2008. *Testing of Chemical Separations Flowsheets for the Global Nuclear Energy Partnership (Genp)-Results from the First "Coupled End-to-End" (Cete) Campaign Using Long-Cooled Lwr Fuel*. Report No. ORNL/GNEP/LTR-2008-038 (OUO), Oak Ridge National Laboratory, Oak Ridge, TN.

Ebert, W, J Cunnane, M Williamson, S Frank, E Buck, D Kolman, E Mausolf, and D Shoesmith. 2010. *Fy2010 Status Report: Developing an Iron-Based Alloy Waste Form*. Report No. AFCI-WAST-2010-000161, Argonne National Laboratory, Argonne, IL.

Ebert, W, J Fortner, I Shkrob, and G Jarvinen. 2009a. *Options for Recovering and Immobilizing the Tc Dissolved During Oxide Fuel Dissolution*. Report No. AFCI-SEPA-PMO-MI-DV-2009-000161, Argonne National Laboratory, Argonne, IL.

Ebert, W, M Williamson, and S Frank. 2009b. *Immobilizing Tc-Bearing Waste Streams in an Iron-Based Alloy Waste Form*. Report No. AFCI-WAST-PMO-MI-DV-2009-000160, Argonne National Laboratory, Argonne, IL.

Gauthier-Lafaye, F, P Holliger, and PL Blanc. 1996. "Natural Fission Reactors in the Franceville Basin, Gabon: A Review of the Conditions and Results of a "Critical Event" in a Geologic System." *Geochimica Et Cosmochimica Acta* 60(23):4831-52.

Kan, HH, RB Shumbera, and JF Weaver. 2008. "Adsorption and Abstraction of Oxygen Atoms on Pd(111): Characterization of the Precursor to Pdo Formation." *Surface Science* 602:1337-46.

Kleykamp, H. 1988. "The Chemical-State of the Fission-Products in Oxide Fuels at Different Stages of the Nuclear-Fuel Cycle." *Nuclear Technology* 80(3):412-22.

Kleykamp, H. 1987. "Composition after Dissolution in $Hno_3$ of the Residue of Knk-Ii-I Fuel." *Atomwirtschaft-Atomtechnik* 32(5):235-36.

Orehotsky, J, and M Kaczenski. 1979. "The Kinetics of the Hydrogen Reduction of $Moo_2$ Powder." *Materials Science and Engineering* 40:245-50.

Prudenziati, M, B Morten, and E Travan. 2003. "Reduction Process Fo Ruo2 Powders and Kinetics of Their Re-Oxidation." *Meterials Science and Engineering* B98:167-76.

Rohatgi, A, and DM Strachan. 2011. *Potential Production Technologies for E-Metal, Tc, and Noble Metals – an Initial Assessment*. Report No. PNNL-20313, Pacific Northwest National Laboratory, Richland, WA.

Schulmeyer, WV, and HM Ortner. 2002. "Mechanisms of the Hydrogen Reduction of Molybdenum Oxides." *International Journal of Refractory Metals & Hard Materials* 20:261-69.

*Standard Density and Volumetric Tables*. 1924. 6th ed., United States National Bureau of Standards, Government Printing Office, Washington.

Strachan, DM, JV Crum, EC Buck, BJ Riley, and MR Zumhoff. 2010. *Fiscal Year 2010 Summary Report on the Epsilon-Metal Phase as a Waste Form for $^{99}tc$*. Report No. FCRD-WAST-2010-000188 (PNNL-19828), Pacific Northwest National Laboratory, Richland, WA.

Strachan, DM, JV Crum, MR Zumhoff, CC Bovaird, J Windisch, C. F., and BJ Riley. 2011. *Epsilon Metal Summary Report Fiscal Year 2011*. Report No. FCRD-WAST-2011-000389, Pacific Northwest National Laboratory, Richland, WA.

Suhonen, S, R Polvinen, M Valden, K Kallinen, and M Harkonen. 2002. "Surface Oxides on Supported Rh Particles: Thermal Decomposition of Rh Oxide under High Vacuum Conditions." *Applied Surface Science* 200:48-54.

Utsunomiya, S, and RC Ewing. 2006. "The Fate of the Epsilon Phase (Mo-Ru-Pd-Tc-Rh) in the $Uo_2$ of the Oklo Natural Fission Reactors." *Radiochimica Acta* 94(9-11):749-53. 10.1524/ract.2006.94.9.749.

Vandegrift, GF. 2009. "Personal Communication "Four-Corners Study Data" (Electronic Spread Sheet Form) "